PHYSICAL REVIEW B **84**, 060403(R) (2011)

Pressure-induced collapse of ferromagnetism in cobalt up to 120 GPa as seen via x-ray magnetic circular dichroism

R. Torchio,[1,2] A. Monza,[3] F. Baudelet,[3] S. Pascarelli,[1] O. Mathon,[1] E. Pugh,[4] D. Antonangeli,[5] and J. Paul Itié[3]

[1]*European Synchrotron Radiation Facility, 6 Rue Jules Horowitz, BP220, F-38043 Grenoble Cedex, France*

[2]*Dipartimento di Fisica, Università di Roma Tre, Via della Vasca Navale 84, Rome, Italy*

[3]*Synchrotron SOLEIL, Saint-Aubin, F-91192 Gif-sur-Yvette, France*

[4]*Cavendish Laboratory, University of Cambridge, Cambridge CB3 0HE, UK*

[5]*Institut de Minéralogie et de Physique de Milieux Condesés, UMR CNRS 7590, Université Pierre et Marie Curie, F-75005 Paris, France*

(Received 5 July 2011; published 18 August 2011)

The magnetism and structure of compressed Co has been studied up to 120 GPa using K-edge x-ray magnetic circular dichroism (XMCD) and x-ray absorption near edge spectroscopy (XANES). The XMCD signal decreases linearly with pressure and is totally suppressed around 120 GPa at ambient temperature. We detect local fcc-like atomic configurations starting from 80 GPa and at 120 GPa these represent at least 40% of the total. Supporting theoretical calculations indicate that the mixed hcp/fcc phase above 120 GPa is nonmagnetic. Comparison between the pressure evolution of magnetism and structure highlights major differences between the Fe and Co cases.

DOI: 10.1103/PhysRevB.84.060403 PACS number(s): 75.50.Cc, 78.20.Ls, 81.40.Vw

The physical properties of the elemental 3*d* transition metals iron, cobalt, and nickel have attracted great interest, in particular for the understanding of magnetism and its influence on the functional properties of metal alloys. The structure and the magnetic properties of these metals are largely determined by the progressive filling of the almost-localized 3*d* orbitals, which also stabilizes the elemental ambient pressure phases: bcc iron, hcp cobalt, and fcc nickel.[1,2] With increasing pressure the hcp and the fcc structures are favored, while the magnetic moment is progressively suppressed.[3–7]

The iron phase diagram has been widely investigated. Being one of the most abundant elements of the Earth's mantle and core, its properties are thought to be intrinsic to various geophysical processes. Upon compression, its ferromagnetic order vanishes around 16 GPa[5–7] in correspondence to the bcc to hcp structural transition and the observation of superconductivity.[8,9]

Similar investigations in the case of cobalt are more challenging due to the higher pressures involved. The ferromagnetic hcp phase is stable over a wide range of pressures, extending from ambient up to around 100 GPa.[10] At high temperature (695 K at ambient pressure), a structural hcp-fcc transition occurs, but the magnetic order is retained up to 1400 K.[3] Under pressure at room temperature, a martensitic hcp-fcc structural phase transition occurs over an extended pressure range, from around 100 GPa to around 150 GPa.[10] The high-pressure fcc phase of cobalt is generally thought to be nonmagnetic, according to the filling factor of the 3*d* electronic band[1] and favored with respect to the hcp-ferromagnetic phase starting from 80–100 GPa.[4,7,10–12] The fcc phase is also the stable structure of nonmagnetic Rh and Ir, the 4*d* and 5*d* isoelectronic elements of Co. Interestingly, an inversion in the pressure evolution of the axial c/a ratio of the hcp phase is reported around 75 GPa,[13] at the same pressure at which anomalies in the elastic and vibrational properties occur.[14,15] *Ab initio* calculations[4,12,15,16] propose a magnetoelastic coupling to be responsible for the observed anomalies. Calculations suggest that hcp-Co compression induces a slow linear reduction of magnetic moment up to 60–80 GPa, above which magnetism is lost more rapidly[4,11,13,17,18] and the c/a ratio of ferromagnetic Co changes pressure derivative, coming to match the c/a ratio of nonferromagnetic hcp-cobalt.[13] Very similar arguments are invoked to explain the softening of the shear moduli and the transverse optical phonon mode, ultimately causing the departure from a linear density dependence of the aggregate elastic moduli and velocities.[9,12,16] The existence of a quantum critical point at 0 K between 100 and 150 GPa and possibly the appearance of a superconducting phase in this vicinity have also been suggested.[4,18] However, despite these numerous experimental and theoretical investigations, which all call to some extent for anomalies in the pressure evolution of the magnetic moment, magnetism of Co at very high pressure is still largely unprobed. K-edge x-ray absorption spectroscopy (XAS) and x-ray magnetic circular dichroism (XMCD) experiments have been performed up to 39 GPa[19] and 100 GPa,[7] without observing complete suppression of the magnetic order. Based on the measured reduction of the XMCD signal, the total disappearance of the magnetic moment in hcp Co was estimated to occur around 150 GPa.[7] Outstanding questions that remain to be answered are, at what pressure is ferromagnetism destroyed in hcp Co, and is its complete suppression necessary to prompt the structural transition to fcc Co, or does the collapse of ferromagnetism spread over the entire pressure range of the structural transition? Thus, our aim was to extend the pressure range for simultaneous structural and magnetic measurements to the complete suppression of ferromagnetism.

We have performed two high-pressure room-temperature XANES and XMCD experiments at the Co K edge ($E_0 = 7709$ eV) on the beamlines ODE (Soleil) and ID24 (ESRF).[20,21] Beam focus sizes were 25×35 and 5×5 μm^2 FWHM, respectively, at the sample position. The pressure range covered was up to 94 GPa on ODE and up to 120 GPa on ID24. Nonmagnetic Be-Cu membrane diamond anvil cells (DAC) of the Chervin design[22] were used with single bevel

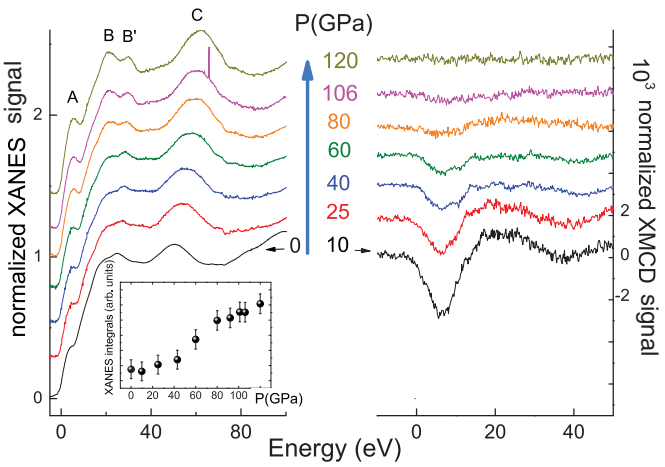

FIG. 1. (Color online) Normalized K-edge XANES (left) and XMCD (right) spectra of cobalt as a function of pressure (ID24). Inset: XANES integral evolution under pressure.

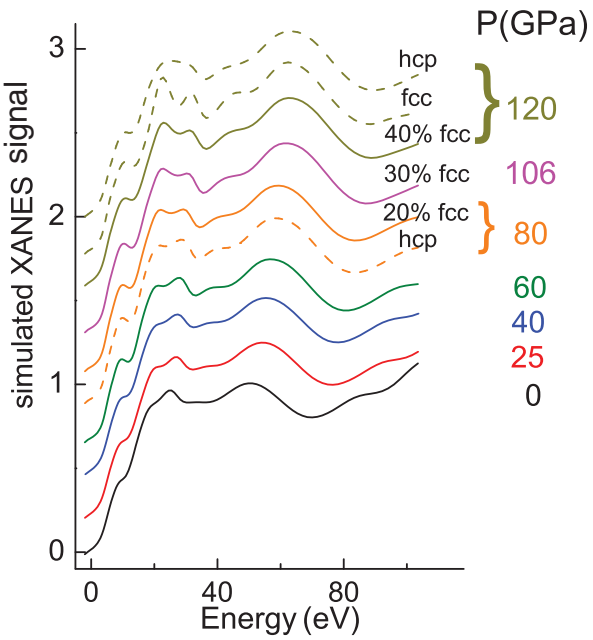

FIG. 2. (Color online) Simulations of XANES spectra using the FEFF code (Ref. 26). The atomic clusters for Co are built using the crystallographic parameters of the structurally distorted hcp and fcc phases found in Refs. 10 and 13. The solid lines are models of our XANES data while the dashed lines show the spectra expected for pure hcp or fcc phases. Above 80 GPa some combined hcp and fcc character is observed in our data.

diamond anvils with 100 μm culets. Fields of 1.3 and 0.7 T were applied at ODE and ID24, respectively; in both cases they were enough to saturate the sample at RT. A rhenium gasket (preindented from 200 μm to around 15 μm thickness) was loaded with the Co sample (4 μm thick high-purity foil 99.9998% from Goodfellow, Ltd.) and a ruby chip. Argon and silicone oil were used as pressure-transmitting media for the ODE and ID24 experiments, respectively. Consistent XANES and XMCD results have been obtained with the two different high-pressure setups, suggesting that different degrees of hydrostaticity did not significantly affect our measurements. The pressure was measured by the ruby fluorescence technique,[23] but as the ruby signal was lost above 80 GPa on ID24 the pressure was also determined using the change in interatomic distances measured by EXAFS (extended x-ray absorption fine structure).[24] Pressure values obtained using both methods (EXAFS and ruby) were found to be consistent.

Figure 1 shows the combined XANES and XMCD data recorded on ID24. The absorption energy range is limited to the XANES and first oscillation of EXAFS. Three features (labeled A, B B′, and C) can be identified. Upon compression, we observe a continuous increase in the intensity of feature A at $E = 4$ eV from the edge (energy of the "dipole forbidden" 1s-3d quadrupole transition). This phenomenon has been reported[7,19,25] for all the 3d metals at high pressure and has been ascribed to the increase in the p character of the d bands (which adds "dipole allowed" intensity to this transition). Pressure indeed favors 3d-4p overlap (hybridization), as the 3d bands widen and the 3d electrons become more delocalized. The double-peak feature B B′ (19 and 24 eV from the edge) changes shape under compression and the relative height of B and B′ is inverted above 80 GPa. Finally the intense peak C, at $E = 50$ eV after the edge, becomes sharper and more pronounced with pressure, while shifting to higher energies as a consequence of compression. In order to better highlight the very subtle modifications induced by pressure in the XANES we integrated the spectra up to half of peak C (inset in left panel of Fig. 1). The integrals show a constant value within the error up to 40 GPa followed by a jump of 4% at 80 GPa, suggesting the onset of a local structural transition. After 80 GPa, the XANES integrals keep increasing continuously, a hint that the transition is not complete at 120 GPa. In order to interpret the evolution of the data with pressure, XANES simulations using the FEFF8 package[26] were performed and are shown in Fig. 2. The atomic Co clusters were built using the crystallographic parameters of compressed hcp and fcc phases found in Refs.[10,13]. Simulations show that main differences in the XANES corresponding to the two phases are visible close to the edge (peaks B and B′) and arise mainly from the changes in the atomic arrangement within the first 5 Å from the absorber (i.e., within the first four shells in the fcc phase). The trend in the experimental XANES data (Fig. 1) can be well reproduced using a pure hcp phase up to about 60 GPa. Starting from 80 GPa the XANES data are better reproduced if the presence of a small fraction of fcc-like atomic configurations is assumed. We estimate that at 120 GPa the fcc phase fraction is at least 40%.[27] This in agreement with the hcp-fcc coexistence pressure range found in x-ray diffraction (XRD) measurements.[10] As illustrated by the top spectrum in Fig. 2, attempts to reproduce the 120 GPa spectrum with a pure hcp structure are definitively unsatisfactory. Nonetheless, a precise evaluation of the fcc/hcp phase fraction cannot be deduced as the intensities of the simulated XANES features also depend on the simulation parameters. The pressure onset for the detection of this phase transition is slightly lower compared to the XRD investigation of Ref. 10, where the onset of the transition was found to occur near 90 GPa (inset of Fig. 2 of Ref. 10). This difference is not a contradiction, since the presence of randomly distributed small (<10 Å) clusters of

newly formed fcc-like Co would be invisible to XRD. Our analysis of the XANES argues for a progressive reduction of the splitting in the first few atomic shells characteristic of the hcp phase of Co, toward the highly symmetric fcc-like phase. These local transformations can be at least qualitatively related to the change in the pressure derivative of the c/a axial ratio[13] and to the anomalies in the elastic moduli[15,16] reported in the literature around 80 GPa. Indeed a reduction of the splitting of the first and third shells of the "nonideal" hcp phase of Co could be detected, from a long-range order perspective, as a small increase in the c/a ratio. Furthermore, *ab initio* calculations[16] indicate a significant softening of the elastic shear modulus c_{44}, which controls the shear strain in the basal plane, starting above ≈75 GPa. As a consequence of this softening, slipping of the basal plane becomes easier, allowing local hcp-to-fcc distortion [in Co the temperature-driven martensitic hcp-to-fcc transition is triggered by 27% softening of c_{44} (Ref. 28)].

The right panel of Fig. 1 presents the XMCD spectra obtained on ID24, normalized to the absorption edge step. The XMCD spectrum consists of a main negative peak (7 eV) followed by a large positive structure (17–24 eV). According to multiple scattering calculations the main negative structure in the Co XMCD spectrum results from the photoelectron scattering by the spin-orbit potential in d and p shells of the neighboring Co atoms.[29]

In Fig. 3, we represent the integral of the absolute value of the XMCD signal, calculated in the energy interval corresponding to the main negative peak, versus pressure (rescaled to the ambient moment value) and comparison with a fit of data and extrapolation from Ref. 7. The data are in very good agreement with Ref. 7 within the error bars up to 100 GPa and complete suppression of the signal is observed at 120 ± 10 GPa. Indeed the collapse of ferromagnetism does not seem to coincide with the complete hcp-fcc structural transformation at 150 GPa,[10] as previously suggested by Ref. 7, but to occur at an earlier stage. On the basis of the present measurements, we point out that the pressure evolution of magnetism and structure in Co reveals major differences with respect to the Fe case. In the latter, ferromagnetism is almost

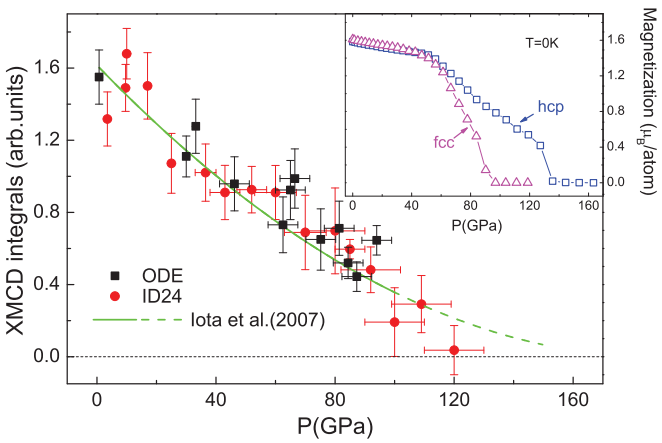

FIG. 3. (Color online) Integral of the K-edge XMCD signal of Co (rescaled to the value of the ambient magnetic moment) in scatter from this work. Solid and dashed lines are fit of data and extrapolation from Ref. 7. The inset shows theoretical calculations of the evolution of the magnetic moment of hcp and fcc cobalt with pressure.

not affected by compression until its abrupt suppression at the bcc-hcp phase transition.[5,7,19] In the former, compression has an immediate effect on ferromagnetism, causing a continuous strong linear decay until total suppression at 120 GPa. Structural modifications starting around 80 GPa do not seem, within our error bars, to affect its evolution.

We have performed density functional calculations (DFTs) to model the pressure dependence of the magnetic moment of hcp and fcc structures of Co. Self-consistent local spin-density approximation calculations were performed using the linear muffin-tin orbital method.[30–32] The 4s and 3d electrons were treated as valence electrons and all others included in the core. The fcc and hcp calculations were performed on a mesh of 897 and 819 k points, respectively, in the irreducible wedge of the Brillouin zone. The calculations give the spin magnetic moment at the corresponding Wigner-Seitz radius of the atoms.[18] Their pressure dependence has been modeled using a semiempirical method utilizing the Birch equation[33] and the experimental data for both the hcp and fcc phases from Ref. 10. The resulting pressure dependence of the magnetic moment is shown in the inset of Fig. 3. The ambient pressure spin magnetic moment from these calculations of 1.59 μ_b compares favorably with the experimental value of 1.58 μ_b.[34]

The calculated magnetic moment of both the hcp and fcc phases decreases with increasing pressure. The initial slow and linear decay in both phases is followed by a more rapid decrease until total suppression at 140 and 90 GPa for the hcp and fcc phase, respectively. Previous calculations[4,11,12,16,17] of the pressure dependence show a qualitative similar trend although there is some variation (≈20%) between these calculations in the values of the critical pressure at which magnetism is suppressed in both the hcp and fcc states.

The main difference between the calculations and the XMCD measurements is that for both hcp and fcc states the calculations show an initial small pressure dependence of the moment followed by a more rapid decrease, whereas our XMCD data show a linear decrease over the whole pressure range within the error bars until complete suppression. It is important to note that the DFT calculations relate to 0 K conditions whereas our XMCD experiments are performed at ambient temperature and probe ferromagnetism. To the best of our knowledge no estimations of the Curie temperature pressure dependence are available in the present range of study; therefore, Curie temperature effects, disrupting the ferromagnetic order, cannot in principle be excluded. Also, the calculations are for either pure hcp or pure fcc phases, while our data show that above ≈80 GPa we enter a mixed hcp/fcc state which has not been modeled by DFT and may be complex in nature.[36] Again, we highlight important differences with respect to Fe. In the latter, the hcp phase into which Fe transforms is predicted to be nonmagnetic long before the phase transition; in Co, the fcc phase into which Co transforms loses its magnetic moment close to the phase transition pressure.[4,7,10–12]

In conclusion, these XMCD and XANES measurements coupled to FEFF and DFT calculations give a complete description of the structural and magnetic Co phase transition which had not been done before, highlighting major differences with the Fe case. A continuous reduction of the XMCD

intensity is observed until complete suppression at 120 ± 10 GPa, providing experimental evidence of pressure-induced extinction of ferromagnetism in Co. In parallel we document a progressive change in the arrangement of the first atomic shells from an hcp- to an fcc-like local structure starting from $P \approx 80$ GPa, providing a coherent scenario which correlates well with elastic[15,16] and structural[13] anomalies reported in the same pressure range. Thus the magnetic response in Co seems to be uniquely affected by compression and not by structural modifications. Our combined experimental and theoretical results support the total disappearance of spin magnetization (local magnetic moment) in the mixed hcp/fcc phase above 120 ± 10 GPa. Nevertheless the different behaviors in the pressure evolution of the theoretical magnetization and XMCD signal decay observed prior to the structural phase transition stimulate further work. The present results thus represent a benchmark for theoretical models addressing the description of extreme-condition physics in the 3*d* metals.

Recently a work by Ishimatsu *et al.*[37] was published describing analogous K-edge XMCD measurements on pure cobalt. In that paper a nonzero signal is reported up to 170 GPa and the authors suggest the existence of an fcc paramagnetic state after 130 GPa. This result is in contradiction to ours and stimulates further experimental work.

E.P. is grateful for support from the Royal Society and we would like to thank G. G. Lonzarich for useful discussions during this work.

[1] H. L. Skriver, Phys. Rev. B **31**, 1909 (1985).
[2] P. Söderlind, R. Ahuja, O. Eriksson, J. M. Wills, and B. Johansson, Phys. Rev. B **50**, 5918 (1994).
[3] C. S. Yoo, , P. Söderlind, and H. Cynn, J. Phys. Condens. Matter **10**, L311 (1998).
[4] G. Steinle-Neumann, L. Stixrude, and R. E. Cohen, Phys. Rev. B **60**, 791 (1999).
[5] O. Mathon, F. Baudelet, J. P. Itié, A. Polian, M. d'Astuto, J. C. Chervin, and S. Pascarelli, Phys. Rev. Lett. **93**, 255503 (2004).
[6] F. Baudelet, S. Pascarelli, O. Mathon, J. P. Itié, A. Polian, M. d'Astuto, and J. C. Chervin, J. Phys. Condens. Matter **17**, S957 (2005).
[7] V. Iota, J. H. P. Klepeis, C. S. Yoo, J. Lang, D. Haskel, and G. Srajer, Appl. Phys. Lett. **90**, 042505 (2007).
[8] K. Shimizu, T. Kimura, S. Furomoto, K. Takeda, K. Kontani, Y. Onuki, and K. Amaya, Nature (London) **412**, 6844 (2001).
[9] E. Pugh, Philos. Trans. R. Soc. London A **361**, 2715 (2003).
[10] C. S. Yoo, H. Cynn, P. Söderlind, and V. Iota, Phys. Rev. Lett. **84**, 4132 (2000).
[11] J. E. Saal, S. Shang, Y. Wang, and Z.-K. Liu, J. Phys. Condens. Matter **22**, 096006 (2010).
[12] P. Modak, A. K. Verma, R. S. Rao, B. K. Godwal, and R. Jeanloz, Phys. Rev. B **74**, 012103 (2006).
[13] D. Antonangeli, L. R. Benedetti, D. L. Farber, G. Steinle-Neumann, A. Auzende, J. Badro, M. Hanfland, and M. Krisch, Appl. Phys. Lett. **92**, 111911 (2008).
[14] A. F. Goncharov, J. Crowhurst, and J. M. Zaug, Phys. Rev. Lett. **92**, 115502 (2004).
[15] D. Antonangeli, M. Krisch, G. Fiquet, J. J. Badro, D. L. Farber, A. Bossak, and S. Merkel, Phys. Rev. B **72**, 134303 (2005).
[16] G. Steinle-Neumann, Phys. Rev. B **77**, 104109 (2008).
[17] T. Jarlborg, Physica C **385**, 513 (2003).
[18] E. Pugh, Ph.D. thesis, University of Cambridge, 1999.
[19] N. Ishimatsu, H. Maruyama, N. Kawamura, M. Suzuki, Y. Ohishi, and O. Shimomura, J. Phys. Soc. Jpn. **76**, 064703 (2007).
[20] S. Pascarelli, O. Mathon, M. Munoz, T. Mairs, and J. Susini, J. Synchrotron Radiat. **13**, 351 (2006).
[21] O. Mathon, F. Baudelet, J. P. Itié, S. Pasternak, A. Polian, and S. Pascarelli, J. Synchrotron Radiat. **11**, 423 (2004).
[22] J. C. Chervin, B. Canny, J. M. Besson, and P. Pruzan, Rev. Sci. Instrum. **66**, 2595 (1995).
[23] H. K. Mao, J. Xu, and P. Bell, J. Geophys. Res. **91**, 4673 (1986).
[24] F. M. Wang and R. Ingalls, Phys. Rev. B **57**, 5647 (1998).
[25] C. R. Natoli, in *EXAFS and Near Edge Structure III* (Springer, Berlin, 1994), p. 167.
[26] A. L. Ankudinov, B. Ravel, J. J. Rehr, and S. D. Conradson, Phys. Rev. B **58**, 7565 (1998).
[27] The coexistence of hcp and fcc Co above 80 GPa is responsible for the larger error on the pressure determination. Compressibility values of the two phases, taken from Refs. 10 and 35, were used to relate changes in interatomic distance to changes in pressure.
[28] B. Strauss, F. Frey, W. Petry, J. Trampenau, K. Nicolaus, S. M. Shapiro, and J. Bossy, Phys. Rev. B **54**, 6035 (1996).
[29] J. P. Rueff, R. M. Galéra, Ch. Giorgetti, E. Dartyge, Ch. Brouder, and M. Alouani, Phys. Rev. B **58**, 12271 (1998).
[30] A program written by S. Froyen and adapted by G. J. McMullan was used to generate the atomic charge densities that were used to calculate the initial potentials.
[31] H. L. Skriver, *The LMTO Method: Muffin-Tin Orbitals and Electronic Structure* (Springer, New York, 1984).
[32] G. J. McMullan, Ph.D. thesis, University of Cambridge, 1989.
[33] F. Birch, J. Geophys. Res. **57**, 227 (1952).
[34] H. P. Meyer and W. Sucksmith, Proc. R. Soc. London A **207**, 427 (1951).
[35] A. Dewaele, M. Torrent, P. Loubeyre, and M. Mezouar, Phys. Rev. B **78**, 104102 (2008).
[36] P. Tolédano, G. Krexner, M. Prem, H.-P. Weber, and V. P. Dmitriev, Phys. Rev. B **64**, 144104 (2001).
[37] N. Ishimatsu, N. Kawamura, H. Maruyama, M. Mizumaki, T. Matsuoka, H. Yumoto, H. Ohashi, and M. Suzuki, Phys. Rev. B **83**, 180409(R) (2011).